Structure and Molecular Weight of the Dynein ATPase

KENNETH A. JOHNSON* and JOSEPH S. WALL‡
*Biochemistry Program, Althouse Laboratory, Pennsylvania State University, University Park, Pennsylvania 16802; and ‡Biology Department, Brookhaven National Laboratory, Upton, New York 11973

ABSTRACT Dynein has been examined by scanning transmission electron microscopy (STEM). Samples of 30S dynein from *Tetrahymena* cilia were applied to carbon films and either were freeze-dried and examined as unstained, unfixed specimens, or were negatively stained with uranyl sulfate. A totally new image of the dynein molecule was revealed showing three globular heads connected by three separate strands to a common base. Two of the heads appeared to be identical and exhibited a diameter of 10 nm while the third head was somewhat larger (~12 nm). The overall length of the particle was 35 nm. Mass analysis, based upon the integration of electron scattering intensities for unstained particles, gave a molecular weight of 1.95 (± 0.24) megadaltons. Mass per unit length analysis was performed using bovine brain microtubules decorated with dynein under conditions where the dynein shows a linear repeat of 24 nm with seven dynein molecules surrounding a microtubule made up of 14 protofilaments. Undecorated microtubules gave a molecular weight per unit length of 21,000 ± 1,900 daltons/Å, compared to a value of 84,400 ± 2,200 daltons/Å for the fully decorated microtubules. Taken together, these data give a molecular weight of 2.17 (± 0.14) megadaltons per dynein molecule, in agreement with measurements on the isolated particles. Mass analysis of individual globular heads observed in isolated particles gave a molecular weight distribution with a mean of 416 ± 76 kdaltons. These data could also be viewed as the sum of two populations of heads with two-thirds of the heads at ~400 kdaltons and one-third at ~550 kdaltons, although more precise data will be required to distinguish two classes of heads with confidence. The mass of the dynein-microtubule complex as a function of distance from the midline of the particle was analysed to distinguish which end of the dynein molecule was bound to the microtubule. The projected mass distribution was consistent with a model where the three dynein heads were oriented toward the microtubule and clearly not consistent with the opposite orientation. These data indicate that the three globular heads form the ATP-sensitive site in this heterologous dynein-microtubule system and suggest that the rootlike base of the dynein molecule forms the structural attachment site to the A-subfiber of the outer doublet in cilia and flagella. The structure and function of the dynein are discussed in terms of these new results.

Dynein is a microtubule-dependent ATPase that drives the sliding of outer doublet microtubules in cilia and flagella (1–4). In these organelles the dynein molecule is structurally attached to the A-subfiber of the outer doublet and interacts transiently with the B-subfiber in an ATP-sensitive manner to couple the hydrolysis of ATP to force production (3, 4). A similar ATPase may interact with cytoplasmic microtubules to provide the force for chromosome movement (5–7) and for other microtubule-dependent motility (8–10). To better evaluate the potential roles of a dyneinlike ATPase in microtubule-dependent motility in general, we consider it important to establish the structure and molecular weight of the ciliary dynein ATPase and to examine the mechanism of its interaction with microtubules and with ATP. Results obtained thus far have progressed toward an understanding of the pathway of ATP hydrolysis (11); however, the structure and the molecular weight of the dynein molecule have yet to be definitively established. Molecular weight estimates, based upon sedimentation equilibrium measurements, have ranged from 1.26 to 5.4 megadaltons (12, 13); whereas, analysis by chemical-quench-flow kinetics has provided an independent measurement of 0.8 to 1.0 megadaltons per ATP binding site (11). Although it has

THE JOURNAL OF CELL BIOLOGY · VOLUME 96 MARCH 1983 669-678

been established that there are two classes of ATPase activity associated with each dynein outer arm in *Chlamydomonas* and sea urchin (14, 15, 16), the exact number of ATP binding sites is not known. Structurally, the dynein molecule has been described as a hook- or a Y-shaped molecule 25 nm in length, as seen in electron micrographs of embedded and sectioned cilia or flagella (17–21). Images of negatively stained outer doublets or isolated dynein, obtained by conventional transmission electron microscopy (TEM), have been interpreted in terms of three or four globular domains connected in series (22), but the relationship of the globular domains to the hook- or Y-shaped structure seen in cross section was not described. Witman and Minervini (23) more rigorously interpreted images of negatively stained outer doublets from *Chlamydomonas* wild type and a mutant lacking the inner arm in terms of a club-shaped dynein arm that is thinner at its point of attachment to the A-subfiber. This view is consistent with the asymmetry of the dynein molecule as seen in cross section; the molecule is thinner toward the end which contacts the A-subfiber to form the structural attachment site and is considerably thicker at the end which interacts transiently with the B-subfiber to form the ATP-sensitive site (17–21). These views are in direct contrast with a recent report in which freeze-fracture techniques provided a view where a thin stalk projected from the globular domains to make contact with the B-subfiber (24).

To resolve the confusion over the structure of the dynein molecule and to overcome the limits of solution hydrodynamic measurements in determining the molecular weight of such a large asymmetric molecule, we have examined dynein by scanning transmission electron microscopy (STEM). STEM has been shown to be a valuable technique in that it allows one to examine protein structure and to simultaneously measure molecular weight (25–29). The detection system of the STEM provides the necessary contrast at low electron dose to permit the visualization of unstained protein molecules and provides a measurement of mass by integration of electron scattering intensities over a particle. This technique is ideally suited to studying dynein because the accuracy and precision of the mass measurement increases as the mass of the particle and because the method does not depend upon shape of the particle. Moreover, because one can directly examine unstained protein, rather than the heavy metals deposited on or around the protein of interest, the technique is free from many of the artifacts of sample preparation. The mass analysis also provides additional information to quantitatively evaluate variables in sample preparation (27) and to help establish the identity of observed particles.

In this report, we demonstrate for the first time that *Tetrahymena* 30S dynein[1] is not a large bulky arm; rather, it is a delicate bouquet of three globular heads, connected by three separate strands to a common base. The molecular weight of the particle is 2×10^6 daltons. Preliminary reports of these data have been presented (30, 31).

MATERIALS AND METHODS

Isolation of Proteins: Dynein was obtained by high salt extraction of cilia from *Tetrahymena thermophila* (strain B-255, a mucus-deficient mutant, was a gift from E. Orias, University of California, Santa Barbara). The cilia were demembranated with 0.25% Nonidet P-40 (NP-40) and were extracted with 0.5 M NaCl, 10 mM HEPES, pH 7.4, 4 mM $MgCl_2$, 1 mM dithiothreitol (DTT) for 30 min at 0°C. The extract was diluted eightfold into 10 mM Tris, pH 8.0, 4 mM $MgCl_2$, 1 mM DTT, and applied to a 5-ml column of DEAE Sephacel (Pharmacia Fine Chemicals, Piscataway, NJ). The dynein was then eluted in a single step with 0.2 M NaCl, 10 mM Tris, pH 8.0, 4 mM $MgCl_2$, 1 mM DTT, then dialysed into 50 mM PIPES, 4 mM $MgCl_2$, pH 7.0, 0.2 mM DTT. This dynein preparation was further fractionated to yield 14S and 30S species by centrifugation on a 5–30% sucrose gradient in 50 mM PIPES, 4 mM $MgCl_2$, 1 mM DTT, pH 7.0. All samples were examined by SDS PAGE as described below.

Microtubule protein was isolated from bovine brain by the method of Murphy and Hiebsch (32). Microtubules were then polymerized by incubation in 50 mM PIPES, pH 7.0, 4 mM $MgCl_2$, 1 mM GTP at 30°C at a protein concentration of 4–8 mg/ml. The microtubules were stabilized by the addition of an equimolar concentration of taxol (1 mol/mol tubulin) (33). The dynein-microtubule complex was prepared by incubation of dynein (0.90 mg/ml) with taxol-stabilized microtubules (0.26 mg/ml) for 20 min at 30°C. The solutions of microtubules or the dynein-microtubule complex were then diluted with 50 mM PIPES buffer to a total protein concentration of 120–150 μg/ml and applied to carbon films for STEM analysis as described below.

SDS PAGE: Samples were examined by SDS PAGE by the method described by Porter (34), using a linear gradient of 5–15% acrylamide and the discontinuous buffer system of Laemmli (35). The cross-linker in the gel system (N_1N^1-methylene-*bis*-acrylamide) was reduced to a concentration equal to 1% of the acrylamide concentration. Chemicals were obtained from Sigma Chemical Co. (St. Louis, MO). Gels were stained with Coomassie Blue by the method of Fairbanks et al. (36).

STEM: Specimens were prepared and imaged at the Brookhaven STEM Biotechnology Resource (25–27) and the procedures for the preparation of carbon films and for specimen application and freeze-drying are described in detail elsewhere (27). Samples of dynein were diluted to 10–30 μg/ml in 10 mM PIPES, 0.8 mM $MgCl_2$, pH 7.0, and applied to a carbon film by injection of 2.5 μl of sample into a 2.5-μl droplet of buffer. The sample was allowed to adsorb to the grid for 30 s and washed four times with 10 mM PIPES buffer. Tobacco mosaic virus (TMV) was added as a standard with the final wash-step in water. The grids were then frozen in nitrogen slush (−210°C) and freeze-dried at constant temperature (−95°C) and pressure (10^{-6} Torr) (see reference 27) and then transferred under vacuum to the microscope stage. Results similar to those described here were obtained when the dynein was applied to the grid in 50 mM PIPES, pH 7.0, or 10–100 mM ammonium acetate, pH 7.0. Parallel samples were negatively stained with 2% uranyl sulfate and allowed to air dry following application of the sample to the grid by the same procedure as outlined above.

Mass Analysis: The data obtained from the STEM were stored in digital form as intensity of electron scattering as a function of position over the grid. These data were then played back to a monitor for photography or for mass analysis (25). The mass analysis was accomplished by integration of electron scattering intensities over an area bounded by the particle minus a background obtained by averaging scattering from areas not containing particles. TMV was used as an internal standard. The dose of electrons for the single scan required to record the data was ≤2 electrons/Å^2 and was sufficiently low to keep mass loss to <1% (25). The use of the internal TMV standard largely compensated for this small degree of mass loss (27).

TEM: Conventional TEM was performed with a Philips EM 300 operated at 60 kV. The dynein-microtubule complex was formed as described above at a ratio of 3 mg dynein/mg tubulin. The complex was then pelleted at 30,000 *g* for 20 min and the supernatant was discarded. The pellet was fixed overnight with 1% glutaraldehyde containing 6% tannic acid (to enhance resolution of the microtubule protofilaments, reference 18) in 50 mM PIPES, pH 7.0, 4 mM $MgCl_2$. The pellets were then postfixed with 1% osmium tetroxide, dehydrated in ethanol, and embedded in Spurr resin. Thin sections (800 Å) were then stained with 2% uranyl acetate.

Computer Modeling of the Projected Radial Mass Distribution: Mass per unit length measurements were performed as a function of increasing diameter about the midline of the dynein-microtubule complex. These data were modeled to determine the orientation of the dynein molecule relative to the microtubule. The modeling was done by assigning an estimated molecular weight to 40 concentric cylinders, 1 nm thick, to define the radial mass distribution of the dynein-microtubule complex. A short computer subroutine was then written to sum over the mass contributions of each cylinder at each diameter of integration. The fraction of the mass per cylinder that contributes to the observed mass is given by $F_i = (2/\pi) \sin^{-1} (D/2R_i)$, where D is the diameter of the area of integration and R_i is the radius of the cylinder. The total mass at each diameter was given by

$$M_D = \sum_{i=1}^{40} F_i M_i,$$

[1] The major dynein species from *Tetrahymena* cilia was originally reported to exhibit a sedimentation coefficient of 30S (12). Recently, Mitchell and Warner (47) have reported a value of 21S based upon calibration of sucrose gradients. We are presently examining *Tetrahymena* dyneins by analytical ultracentrifugation, but we will continue to refer to the faster sedimenting species as 30S, until the sedimentation coefficient has been definitively established.

where M_i is the mass contained within the i^{th} cylinder and the sum is taken over all cylinders.

The assignment of mass for each cylinder was based upon the known structure of the microtubule wall (37) and the molecular weights of the elements of the dynein molecule described here. The microtubule contributed a molecular weight per unit length of 14 × 110 kdaltons/80 Å that was distributed over a radius of 7–13 nm. The dynein heads contributed 7 × 1.3 megadaltons/240 Å; the stems, 7 × 500 kdaltons/240 Å; and the base, 7 × 400 kdaltons/240 Å. For the model with the heads oriented toward the microtubule, the mass due to the heads was distributed over the radius of 14–24 nm, the stems over the radius of 25–32 nm, and the base over the radius of 33–40 nm. This assignment was inverted to consider the opposite orientation of the dynein. Changes in the actual distribution of this mass within each range did not alter the general shape of the curve; only the bumpiness of the curve was affected. In addition, errors in the position of the midline, which was chosen somewhat arbitrarily in performing the analysis, did not alter the general trend. Modeling studies showed that, if the midline was within the central hollow core of the microtubule (±4 nm of actual center), the general shape of the curve was not affected. Since the fitted curves were largely independent of the choice in the midline and the actual distribution of mass within each domain (head, stem, or base region), the fit is not a function of arbitrary choices in these parameters. One can confidently distinguish models involving opposite orientations of the dynein molecule, since these models predict markedly different radial mass distributions.

RESULTS

Characterization of the Dynein Preparation

The dynein used in this study was obtained by high salt extraction of *Tetrahymena* cilia and was purified by chromatography on DEAE Sephacel and by sedimentation on a sucrose gradient to yield the 30S dynein species. This preparation has been extensively studied and is the most pure and biologically active *Tetrahymena* dynein preparation available in terms of its ability to quantitatively rebind to microtubules and to catalyse a stoichiometric presteady-state phosphate burst (11, 38). The major potential problem with dynein preparations from *Tetrahymena* is the digestion of dynein heavy chains by endogenous proteases. Our efforts to minimize the potential for proteolysis include extensive washing of the cilia in the presence of phenylmethylsulfonyl fluoride (PMSF) and EGTA before and after demembranation and rapid column purification of the dynein following extraction (11). In addition, all samples for STEM analysis were examined within 36 h of the start of the preparation procedure, and SDS PAGE was used to check for possible proteolysis. Fig. 1 (*left* lane) shows the results of a typical gel sample, illustrating the predominant heavy chain. The right lane shows the same sample greatly overloaded to reveal the minor components. As originally described by Porter and Johnson (38), this dynein preparation consists of 3 heavy chains (~400 kdalton), which are not resolved on this gel system, two to three intermediate chains (70–100 kdalton), and a small number of light chains (15–20 kdalton). There are a few minor bands between the heavy and intermediate chains, but they are present in far less than stoichiometric amounts relative to the heavy and intermediate chains. This pattern is indicative of a good preparation showing no significant proteolysis.

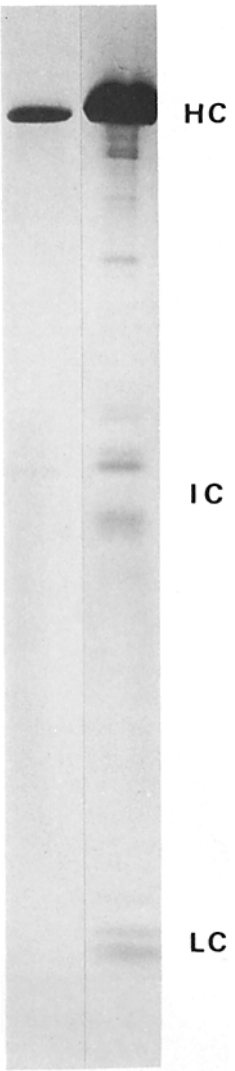

FIGURE 1 SDS PAGE analysis. *Tetrahymena* 30S dynein was analysed by SDS PAGE as described in Materials and Methods.

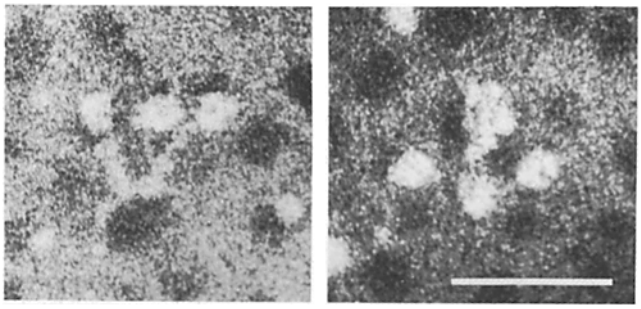

FIGURE 2 The structure of 30S dynein. 30S dynein was diluted to 30 μg/ml, applied to a carbon-coated holey grid, washed four times with 10 mM PIPES buffer, pH 7.0, and negatively stained with 2% uranyl sulfate. Bar, 50 nm. × 425,000.

Structure and Molecular Weight of Dynein

Dynein was applied to carbon films and freeze-dried for examination of unstained specimens for mass and structural analysis, and parallel samples were negatively stained as described in Materials and Methods. Fig. 2 shows 30S dynein negatively stained with 2% uranyl sulfate and viewed in the STEM. These micrographs clearly show three globular heads, joined by three strands to a common base. The overall length of the molecule is 35 nm and each globular head has a diameter of ~10 nm. Two of the heads appear to be identical while the third head is somewhat larger and is connected by a thicker strand. The base of the molecule in the left-hand image appears to be open, suggesting a rootlike structural attachment site, whereas in the image on the right the base exhibits a more compact view. These overall views, showing three or four globular domains, are seen repeatedly in stained and unstained specimens, although not every particle exhibits this morphology.

The question of heterogeneity of the sample is best addressed by analysis of unstained specimens because of the additional information provided by the mass analysis. Fig. 3 shows the dark-field image obtained with unstained, unfixed 30S dynein, applied to a carbon film and freeze-dried. One sees several molecules that conform to the three-headed bouquet arrangement and several molecules which could be interpreted as a different arrangement of the same units, formed as the protein adsorbed to the carbon film. The mass analysis is particularly valuable in that it allows one to address the question as to whether the apparently different morphologies represent particles with the same mass.

The observed structures and masses of various particles are shown in Fig. 4. The number listed beneath each particle is its mass in megadaltons. The particles have been grouped in the upper row as those that conform to the three-headed bouquet arrangement and in the lower row as those that exhibited a somewhat different view. As can be seen by inspection of these numbers, the molecular weights of all particles are the same within the limits of error in the measurement.

A histogram describing the masses of all particles measured is shown in Fig. 5. These data show a predominant peak at 1.95 megadaltons with a standard deviation of the mean of 12% (n = 85). In addition, one can see a peak at twice this value, 3.8 megadaltons, that presumably represents dimers of the dynein molecule; visual inspection of particles exhibiting a mass of 3.8 megadaltons supports this conclusion. Some higher order aggregates can be seen in Fig. 3, but these were excluded from the analysis. Identification of the monomeric protein unit is potentially a problem. One expects to observe dimers of the parent molecular weight due to the finite probability that two particles will adsorb at or near the same location on the grid. Therefore, observations of particles at 3.8 megadaltons supports the identification of the 1.95-megadalton particle as the parent molecule.

The theoretical limit of error in the mass measurement, due to counting statistics and substrate thickness variation, is 4.3% for a 2-megadalton particle covering a 700-Å diameter area of the grid. The observed error of 12% may be due to heterogeneity in the sample or the background; further work is aimed at refining the sample preparation procedure to distinguish these alternatives.

The identity of the 1.95-megadalton particle can be more unequivocally addressed by mass per unit length analysis of the dynein-microtubule complex. Previous work in this laboratory has established conditions for the formation of a complex between 30S dynein and bovine brain microtubules, and titration experiments have shown that the microtubule sites are

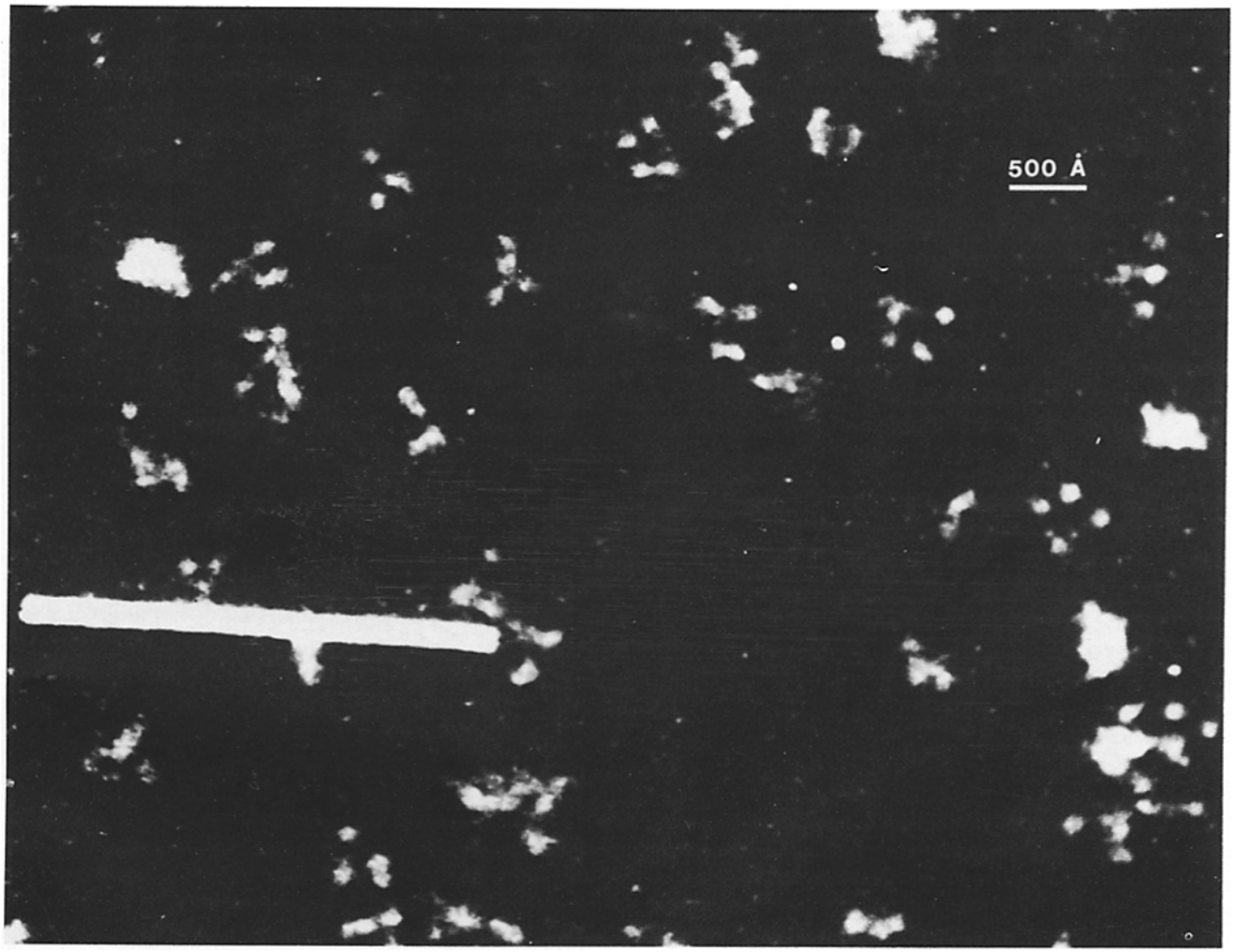

FIGURE 3 Unstained dynein observed in the STEM. 30S dynein was diluted to 30 μg/ml and applied to a carbon film and freeze-dried as described in Materials and Methods, then examined in the STEM. The long rod is a TMV particle used as an internal standard for the mass analysis. × 220,000.

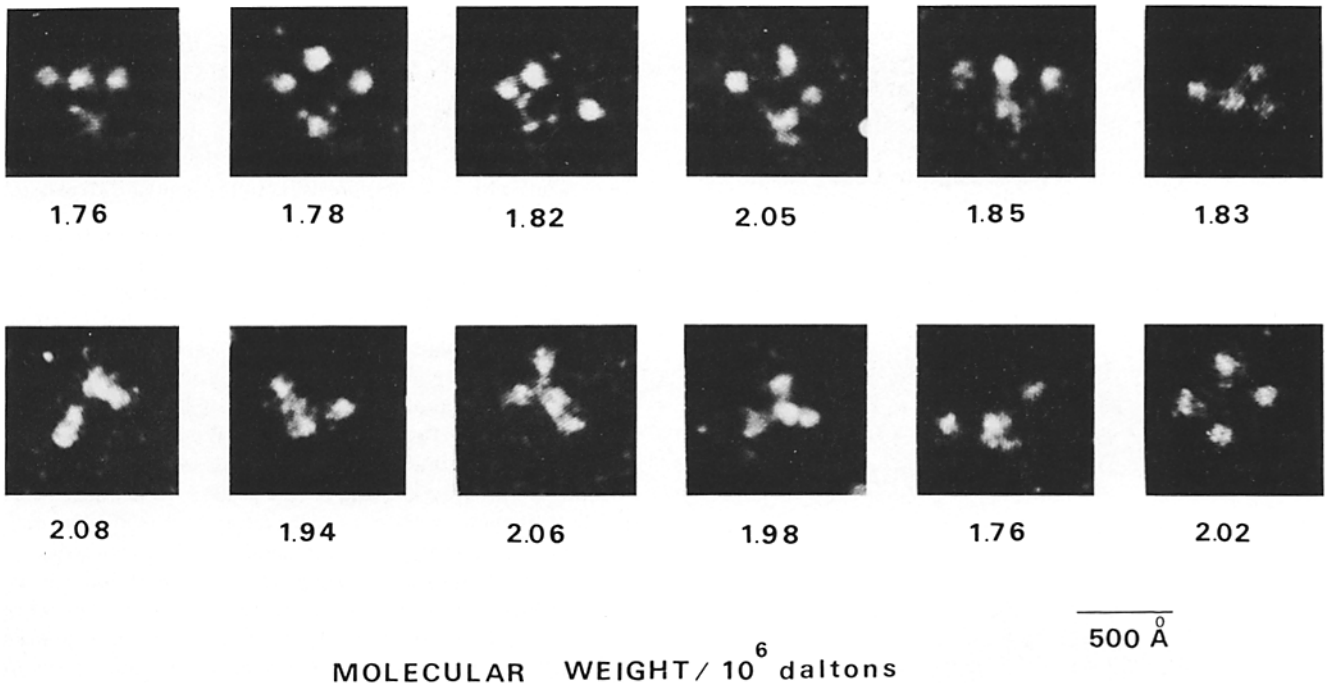

FIGURE 4 Mass analysis of individual particles. Samples were prepared as described in the legend to Fig. 3. For each image shown here, the mass of the particle in millions of daltons is given beneath the particle. × 260,000.

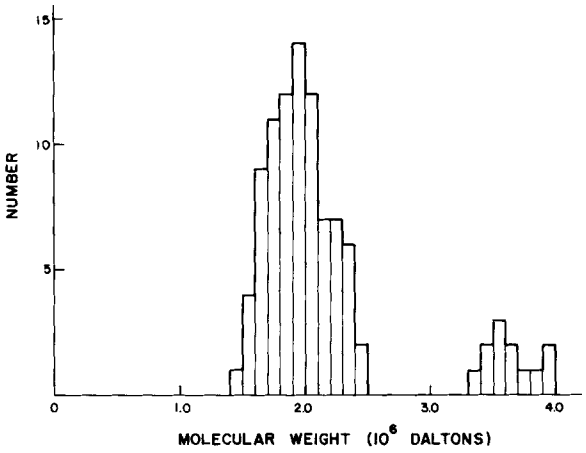

FIGURE 5 Histogram of molecular weights of isolated particles. Molecular weights were determined by integration of electron scattering intensities over each particle. The molecular weight distribution is shown for a total of 97 particles measured. The predominant peak gives a molecular weight of 1.95 ± 0.24 for 88% of the particles.

saturated at a ratio of 3 mg dynein/mg tubulin (38). Analysis by TEM has shown that the dynein exhibits a 24-nm repeat along the axis of the microtubule (38), and in cross section there are seven dynein molecules surrounding a microtubule containing 14 protofilaments as shown in Fig. 6. These numbers alone suggest a molecular weight of 2.0 megadaltons, but the accuracy of the titration data may be subject to some question since it relies upon measurement of protein concentration and it includes terms for the fractions of dynein and tubulin which are active. Mass per unit length analysis of the dynein-microtubule complex circumvents these problems by looking only at the protein bound to the microtubule and provides an independent measurement of mass, averaged over many dynein molecules. More importantly, the monomeric dynein molecule is now defined as the biochemically active component decorating microtubules with a 24-nm repeat as described by several authors (20, 38, 40–42). Fig. 7 shows unstained, freeze-dried samples of microtubules and the dynein-microtubule complex observed in the STEM. Mass per unit length measurements gave values of 21.0 ± 1.9 kdaltons/Å (n = 33) for the microtubule and 84.4 ± 2.2 kdaltons/Å (n = 8) for the dynein-microtubule complex. Based upon the repeat of seven dyneins per 24 nm, these data gave a molecular weight of 2.17 ± 0.14 megadaltons per dynein molecule. This is in agreement with the mass measurements on individual dynein molecules, within the limits of error.

The somewhat higher value of the molecular weight resulting from analysis of the dynein-microtubule complex may be due to unpolymerized tubulin and excess dynein that were not removed from the dynein-microtubule complex before sample preparation. A random distribution of unpolymerized protein over the surface of the grid would not be subtracted by the background calculation and would therefore contribute to the mass of the dynein-microtubule complex. Nonetheless, the relatively intense electron scattering by the dynein-microtubule complex allows for accurate mass measurement with only negligible contribution of the background protein and the slight increase in molecular weight over that observed for isolated particles is deemed to be insignificant.

Molecular Weight of the Heads

We have also used the STEM to dissect the dynein molecule by making mass measurements on each globular head for those molecules where the heads were well separated. A histogram showing the results of this analysis is given in Fig. 8. The data could be interpreted in terms of a single class of heads with a mass of 416 ± 76 kdaltons. Alternatively, the data could be viewed as the sum of two populations with two-thirds of the heads exhibiting a molecular weight of ~400 kdaltons and one-

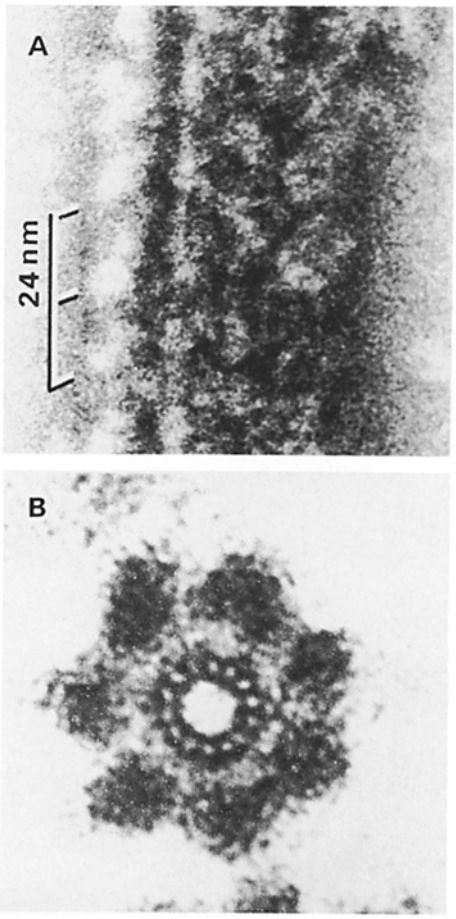

FIGURE 6 The structure of the dynein-microtubule complex. (*A*) A dynein-microtubule complex was prepared at a ratio of 3 mg dynein/mg tubulin and applied to a carbon film and negatively stained with 2% uranyl sulfate, then imaged with the STEM. (*B*) The dynein-microtubule complex was fixed, embedded, and cross sectioned as described in Materials and Methods, and viewed by TEM. × 500,000.

third having a molecular weight of ~550 kdaltons. This latter interpretation is supported by the negatively stained images and by mass analysis of those molecules where all three heads could be measured. However, these data are only suggestive, and further work is required to establish the molecular weight of the heads with sufficient precision to distinguish two classes.

Orientation of the Dynein Relative to the Microtubule

The asymmetry of the dynein molecule, as seen in fixed, embedded and cross-sectioned cilia, suggests that the rootlike base of the bouquet forms the structural attachment site (A-subfiber binding) and that the three globular heads form the ATP-sensitive site (B-subfiber binding). We have more closely examined the dynein-microtubule complex to address the identification of the structural and ATP-sensitive sites of the dynein molecule. Previous work in this laboratory has established that, under our conditions in vitro, dynein associates with bovine brain microtubules via the ATP-sensitive site (reference 38, and manuscript in preparation); therefore, the present work serves to define the orientation of the dynein molecule opposite to the normal structural binding of dynein to the A-subfiber of the outerdoublet.

Examination of fixed, embedded, and sectioned samples (Fig. 6 *B*) does not allow for a rigorous analysis of the distribution of protein around the microtubule, due to complications introduced by the sectioning and staining procedure. For example, one sees the microtubule protofilaments negatively contrasted whereas the dynein is positively stained. What appears to be a space between the dynein and the microtubule may be a function of the shift between positive and negative staining and the build-up of tannic acid around the microtubule. In addition, one must consider that the sections are of a thickness equal to three dynein molecules and that the most intense staining of the heads may anomalously appear to be farther away from the points of contact with the microtubule.

The radial distribution of protein around the microtubule can be better determined by mass analysis of the dynein-

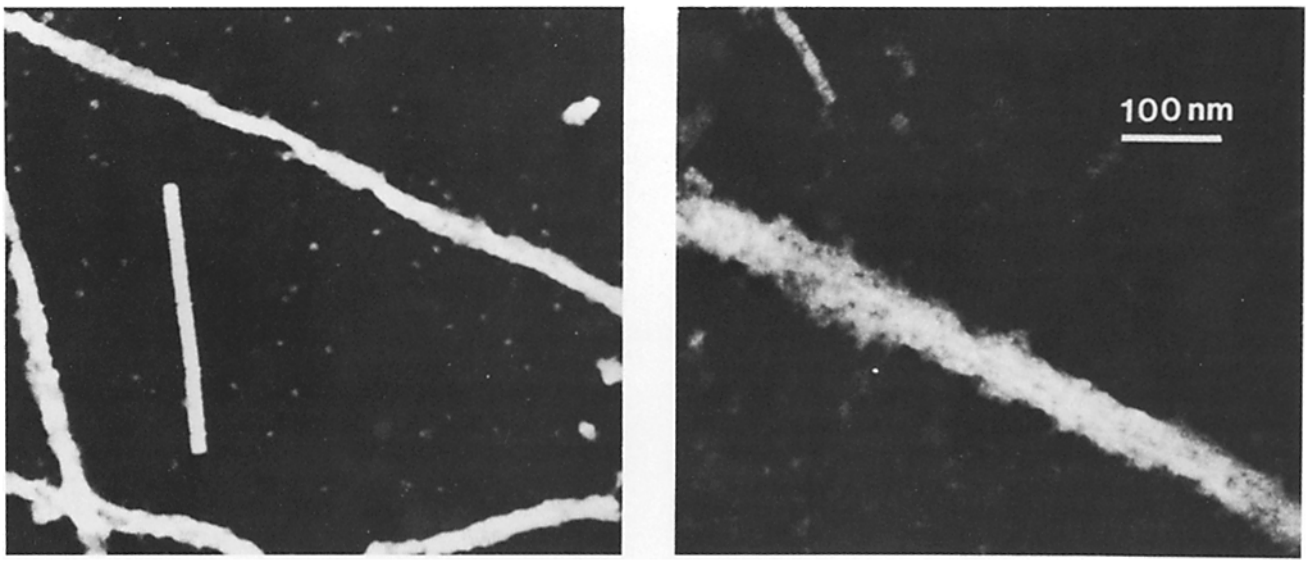

FIGURE 7 Mass analysis on the dynein-microtubule complex. Microtubules (*left*) and dynein-microtubule complex (*right*) were prepared and examined as unstained specimens in the STEM. The shorter rods in each micrograph are TMV particles. × 130,000.

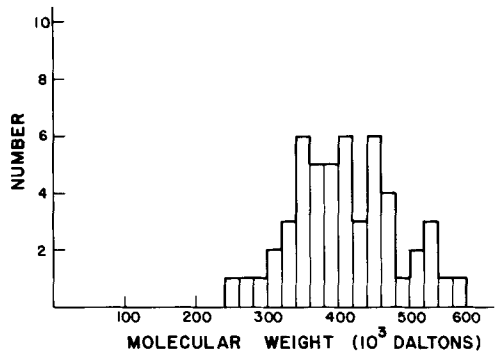

FIGURE 8 Histogram of molecular weights of the individual heads. Mass analysis was performed to determine the molecular weight of each globular head for those particles where the heads were well separated, as described in Materials and Methods. The figure shows the molecular weight distribution for 57 heads.

microtubule complex in unstained preparations. The mass per unit length was measured as a function of increasing radius of integration about the midline of the microtubule to obtain the data shown in Fig. 9. The lower figure shows the integrated molecular weight as a function of radius while the upper figure shows the derivative curve, the change in mass with the change in radius of integration. By this analysis, one effectively performs serial longitudinal cross sections through a single dynein-microtubule complex by computation of the mass of protein in each section as a function of increasing radius from the midline of the projected image. This projected radial mass distribution is a sensitive function of the orientation of the dynein molecule relative to the microtubule and can readily distinguish whether the heads are oriented toward or away from the microtubule. The solid line (Fig. 9) represents the results expected for a model where the dynein heads are oriented toward the microtubule and the dashed line describes the results expected for the opposite orientation. The features of the data which allow one to distinguish these models are most clearly shown in the derivative curve. By either model there is a rapid increase in mass between 4 and 12 nm as one sections through the microtubule wall. If the heads are oriented toward the microtubule, one expects a continued increase in mass between 12 and 22 nm; whereas, if the heads are oriented away from the microtubule, the second large increase in mass should occur at a greater radius, between 24 and 34 nm. The fit to the data is clearly better for the model where the heads are oriented toward the microtubule. Moreover, the model with the heads oriented away from the microtubule predicted a curve far outside the limits of error in the measurement. (See Materials and Methods for a discussion of the fitting method.) Models which included a 2-nm space of reduced mass between the microtubule and the dynein head (Fig. 6 *B*) predicted a large dip in the derivative curve between 12 and 14 nm that is not evident in the data (calculated curve not shown). These quantitative data provide evidence that the three globular heads contain the sites for the ATP-sensitive binding of dynein to the microtubule in this heterologous system and suggest that the base of the bouquet forms the structural attachment site on the outer doublet.

DISCUSSION

Tetrahymena 30S dynein is uniquely suited for structural and kinetic analysis. Dyneins from *Chlamydomonas* and *Tripneustes* (sea urchin) break down to form smaller particles upon extraction (39) or upon dialysis to lower ionic strength buffers (15), respectively; whereas, purified *Tetrahymena* 30S dynein is stable over a wide range of ionic strengths (unpublished data). In addition, *Tetrahymena* 30S dynein retains its ability to bind to microtubules via both its structural attachment site and its ATP-sensitive site (20, 38, 40–42). It thus appears that the isolated *Tetrahymena* 30S dynein is a complete molecule in that it retains these two essential microtubule binding sites in addition to the ATPase site(s). Moreover, because large volumes of *Tetrahymena* can be grown on a simple, inexpensive medium, quantities of dynein can be obtained that are sufficient for transient state kinetic analysis (11).

The studies presented here demonstrate for the first time that the *Tetrahymena* 30S dynein molecule consists of three independent globular heads attached by three separate strands to a common base and provide a unique measurement of molecular weight. Structural and kinetic information obtained to date and interpreted in terms of a single rather bulky arm must now be reinterpreted in terms of this new structure.

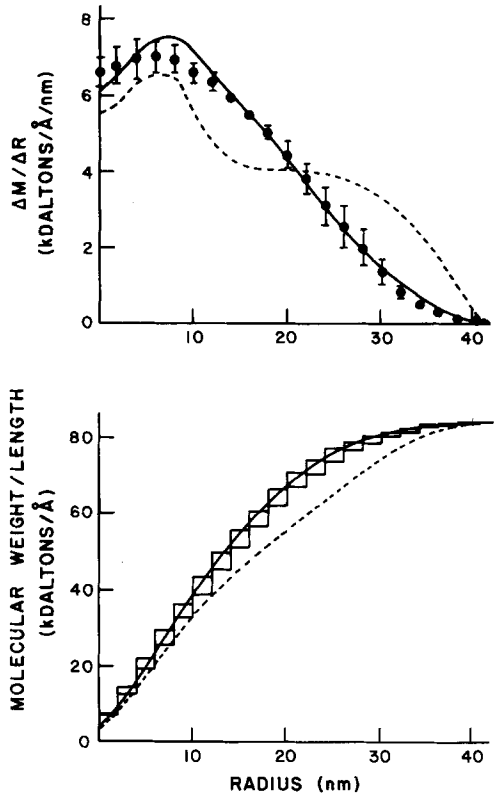

FIGURE 9 Projected radial mass distribution of the dynein-microtubule complex. The mass per unit length of the dynein-microtubule complex was determined by integration of electron scattering intensities as described in Materials and Methods. Successive measurements were made with increasing diameter about the midline of the particle to obtain the results shown in the lower figure. The upper figure shows the derivative, or the increment of increase in molecular weight with increasing radius. The data are the averages of results obtained for three particles examined in detail, and the error bars show the standard deviation of the mean. In the lower figure the data are plotted as a bar graph showing the upper and lower limits of error. The solid line is a theoretical curve calculated for a model where the three dynein heads are oriented toward the microtubule, whereas the dashed line was calculated for the model with the heads oriented away from the microtubule (see Materials and Methods).

We must consider at this point whether our three-subunit bouquet model can account for previous images of the dynein arm observed in situ. Our analysis of the projected radial mass distribution of the dynein-microtubule complex argues that the rootlike base of the bouquet forms the site for structural attachment to the A-tubule of the outer doublet and that the three independent heads interact with the B-subfiber in a reaction coupled to the hydrolysis of ATP to produce the force for sliding. Previous models of the dynein outer arm are summarized in Fig. 10 in comparison to the model described here. Originally, Allen (17) described the *Tetrahymena* dynein outer arm as an asymmetric, hook-shaped molecule, based upon his observations of fixed and sectioned axonemes. This low-resolution view, resulting from the superposition of approximately three dynein arms in cross section, is clearly consistent with our model. Subsequently, Warner et al. (22) described the dynein arm as a three-subunit rod, based upon his observations of negatively stained *Tetrahymena* outer doublets and isolated dynein by conventional TEM. However, the contrast in his images was barely sufficient to resolve the three globular units and would not have been sufficient to resolve the strands connecting the heads to the base. In general, Warner's original observation of three globular units is in agreement with our model, although we present a markedly different arrangement of those units to form the arm. Witman and Minervini (23) more rigorously analysed images of negatively stained outer doublets from *Chlamydomonas* and described a club-shaped arm, which clearly supports our structural assignment. Finally, in work that was done concurrently with the present study, Heuser and Goodenough (24) also observed three globular subunits in replicas of frozen, deep-etched, rotary-shadowed axonemes from both *Chlamydomonas* and *Tetrahymena*. However, they have suggested that two of the subunits are "feet" that associate with the A-tubule and support the third subunit that is attached to the B-subfiber via a stalk. This rather puzzling view led Heuser and Goodenough (24) to postulate that existing models of the ciliary stroke may be backwards and that the dynein may be structually attached to the B-subfiber. Naively, one might suggest that the roots of our three-subunit bouquet should be attached to the B-subfiber to account for this interpretation. However, our observations indicate that the strands connecting the heads to the base of the bouquet are quite flexible and that the most rational explanation of the images obtained by the freeze-etch procedure would be that the three heads collapse back onto the A-subfiber during the etching process and therefore only appear to be associated directly with it. Accordingly, the stalk observed in the freeze-etch images may be a new structure, independent of the dynein arm, and could serve to resist the sliding movements in a manner analogous to the postulated roles for the interdoublet links near the inner arm (17, 21).

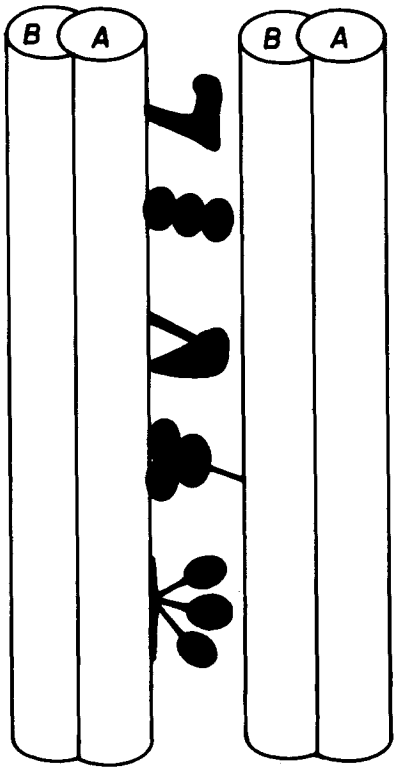

FIGURE 10 Models of the dynein arm. Schematic representations of various models of the dynein arm. Upper to lower: hook described by Allen (17); three-subunit rod described by Warner et al. (22); club described by Witman and Minervini (23); three-subunit mouse described by Heuser and Goodenough (24); and three-headed bouquet described here.

In general, the images observed in situ support our model of the ciliary dynein outer arm in terms of the well-established asymmetry of the arm and the observation of three subunits. Other models differ only in the interpretation of the images, and we should stress that the three-subunit bouquet model is based upon data at much higher resolution and provides a new way of looking at the dynein molecule that affords a reasonable interpretation of all images obtained in situ. Further analysis of the intact outer doublets by STEM will be required to more definitively localize the elements of the bouquet.

In collaboration with George Witman, we have examined *Chlamydomonas* 12S and 18S dyneins by STEM (43). These studies have shown that the 18S particle consists of two heads connected by two strands to a base and exhibits a mass of 1.25 megadaltons; each head has a mass of 380 kdaltons. The 12S particle was a single globular unit with a mass of ~500 kdaltons. Thus, the structures and the masses of the 12S and 18S particles form *Chlamydomonas* sum to be nearly equal to that observed for the *Tetrahymena* 30S dynein. In addition, the polypeptide composition of the *Tetrahymena* dynein corresponds to the sum of the polypeptide compositions of the *Chlamydomonas* dyneins. *Chlamydomonas* 18S dynein consists of two heavy chains (320 and 300 kdaltons), two intermediate chains (86 and 73 kdaltons), and eight light chains (15–18 kdaltons [39]). The 12S particle consists of one heavy chain (315 kdaltons) and one light chain (19 kdaltons). *Tetrahymena* 30S dynein consists of three heavy chains, two intermediate chains, and six light chains that approximately co-migrate with the *Chlamydomonas* 18S and 12S polypeptides combined (Pfister, Witman and Johnson, unpublished results). The combination of the STEM analysis and the SDS PAGE analysis provides strong confirmation of the three-headed bouquet model. Moreover, these data reinforce our suggestion that one of the heads is larger than the two apparently identical heads and indicate that there must be ATPase activity in the third, larger head as well as in the domains defined by the 18S dynein.

The data on *Tetrahymena* and *Chlamydomonas* quite convincingly demonstrate that the dynein outer arm from these sources consists of a three-headed bouquet. However, current data on sea urchin 21S dynein would seem to indicate that the dynein outer arm is a two-headed molecule. Yano and Miki-Noumura (19) described the sea urchin 21S dynein as a two-headed or heart-shaped molecule. Although the resolution in their images was not good enough to be entirely convincing, the molecular weight measurement of 1.26 megadaltons (12) and the observation of only two rather than three heavy chains (44) would seem to support a two-headed model. In addition, digestion of sea urchin dynein has resulted in a subfragment

with ATPase activity and a molecular weight of 400 kdaltons (44), corresponding to the mass of the two identical heads observed in *Tetrahymena* 30S and in *Chlamydomonas* 18S dyneins. It is interesting to speculate that a three-headed dynein is required to generate a ciliary waveform in *Tetrahymena* and *Chlamydomonas*; whereas, a two-headed dynein is sufficient for generation of a flagellar waveform in sea urchin. Further analysis of the function of the three dynein heads and analysis of sea urchin 21S dynein by STEM will be required to resolve these questions.

Our rapid chemical-quench flow experiments have shown that *Tetrahymena* dynein exhibits a presteady-state phosphate burst (11). The amplitude of the ATP binding transient provides an independent measurement of the molecular weight per ATP site. Measurements to date have given a mass of 0.8–1.0 megadaltons per ATP site, suggesting that there are 2–2.5 ATP sites per dynein arm. More precise measurements will be required to establish whether there are two or three ATP sites per dynein that exhibit a presteady-state phosphate burst. An intriguing alternative is that the two identical heads each exhibit a phosphate burst and are involved in normal force production. The third larger head, corresponding to the *Chlamydomonas* 12S ATPase, may not show a phosphate burst under our conditions but may respond to regulate the cilium.

We have only just begun to exploit the wealth of information provided by the STEM analysis. The STEM mass analysis is the method most suited for the determination of molecular weight of a large asymmetric molecule such as dynein and is not subject to the kinds of errors that hinder analysis by sedimentation equilibrium. Moreover, the STEM allows one to measure the masses of different domains of the same structure and to simultaneously view isolated particles with better resolution and contrast than obtainable by conventional TEM. Further analysis is aimed at localization of the polypeptides and the ATP and microtubule binding sites in terms of the elements of the bouquet.

It should be noted that the mass per unit length measurement on the microtubules provides the first definitive evidence that each globular unit in the microtubule lattice is either an α or a β subunit and not an $\alpha\beta$ dimer. The mass analysis provides a measurement of 51,000 ± 4,800 daltons/40-Å globular unit if one accounts for the MAPs (15% of total protein) and for 14 protofilaments per tubule, in agreement with the molecular weights of tubulin based upon the amino acid sequence (48, 49). Previous analysis relied upon measurements of the size of the globular unit seen by TEM in negative stain and estimates of the mass of protein which could be fit into that unit (37, 45, 46). The present work demonstrates unequivocally that the previous analysis gave the right answer.

The authors wish to thank James Hainfeld for sharing his expertise and Kristin Chung, Tom Doman, Ed Desmond and Frank Kito for their outstanding technical assistance.

The work presented here was performed at the Brookhaven STEM, a National Institutes of Health Biotechnology Resource (RR00715).

Supported by National Institutes of Health grant GM26726 (to K. A. Johnson).

Received for publication 3 May 1982, and in revised form 12 October 1982.

REFERENCES

1. Summers, K. E., and I. R. Gibbons. 1971. Adenosine triphosphate-induced sliding of tubules in trypsin-treated flagella of sea urchin sperm. *Proc. Natl. Acad. Sci. U.S.A.* 68:3092–3096.
2. Satir, P. 1968. Studies on cilia III. Further studies on the cilium tip and a "sliding filament" model of ciliary motility. *J. Cell Biol.* 39:77–94.
3. Brokaw, C. J., and B. Benedict. 1968. Mechanochemical coupling in flagella. I. Movement-dependent dephosphorylation of ATP by glycerinated spermatozoa. *Arch. Biochem. Biophys.* 125:770–778.
4. Gibbons, B. H., and I. R. Gibbons. 1972. Flagellar movement and adenosine triphosphatase activity in sea urchin sperm extracted with Triton X-100. *J. Cell Biol.* 54:75–97.
5. Cande, W. Z., and S. M. Wolniak. 1978. Chromosome movement in lysed mitotic cells is inhibited by vanadate. *J. Cell Biol.* 79:573–580.
6. Pratt, M. M., T. Otter, and D. Salmon. 1980. Dynein-like Mg^{+2}-ATPase in mitotic spindles isolated from sea urchin embryos (*Strongylocentrotus droebachiensis*). *J. Cell Biol.* 86:738–745.
7. Inoué, S. 1981. Cell division and the mitotic spindle. *J. Cell Biol.* 91(3, Pt. 2):131s–147s.
8. Mooseker, M. A., and L. G. Tilney. 1973. Isolation and reactivation of the axostyle: evidence for a dynein-like ATPase in the axostyle. *J. Cell Biol.* 56:13–26.
9. Forman, D. S. 1981. A permeabilized cell model of saltatory organelle movement. *J. Cell Biol.* 91(2, Pt. 2):414*a*. (Abst.).
10. Beckerle, M. C., and K. R. Porter. 1982. Inhibitors of dynein activity block intracellular transport in erythrophores. *Nature (Lond.).* 295:701–703.
11. Johnson, K. E., and M. E. Porter. 1982. Transient state kinetic analysis of the dynein ATPase. *Cell Motility.* 1(Suppl.):121–106.
12. Gibbons, I. R., and E. Fronk. 1979. A latent adenosine triphosphatase form of dynein 1 from sea urchin sperm flagella. *J. Biol. Chem.* 254:187–196.
13. Gibbons, I. R., and A. J. Rowe. 1965. Dynein: a protein with adenosine triphosphatase activity from cilia. *Science (Wash. DC).* 149:424–425.
14. Huang, B., G. Piperno, and D. J. L. Luck. 1979. Paralysed flagella mutants of *Chlamydomonas reinhardtii* defective for axonemal doublet microtubule arms. *J. Biol. Chem.* 254:3091–3099.
15. Tang, W. Y., C. W. Bell, W. S. Sale, and I. R. Gibbons. 1981. Structure of the dynein-1 outer arm in sea urchin sperm flagella I. Analysis by separation of subunits. *J. Biol. Chem.* 257:508–515.
16. Fay, R. B., and G. B. Witman. 1977. The localization of flagellar ATPases in *Chlamydomonas reinhardtii. J. Cell Biol.* 75(2, Pt. 2):286*a*. (Abstr.)
17. Allen, R. D. 1968. A reinvestigation of cross-sections of cilia. *J. Cell Biol.* 37:825–831.
18. Tilney, L. G., J. Bryan, D. J. Bush, K. Fujiwara, M. S. Mooseker, D. B. Murphy, and D. H. Snyder. 1973. Microtubules: evidence for 13 protofilaments. *J. Cell Biol.* 59:267–275.
19. Yano, Y., and T. Miki-Noumura. 1981. Two-headed dynein arm. *Biomed. Res.* 2:73–78.
20. Haimo, L. T., B. R. Telzer, and J. L. Rosenbaum. 1979. Dynein binds to and crossbridges cytoplasmic microtubules. *Proc. Natl. Acad. Sci. USA.* 76:5759–5763.
21. Gibbons, I. R. 1975. The molecular basis of flagellar motility in sea urchin spermatozoa. *In* Molecules and Cell Movement. S. Inoué and R. E. Stephens, editors. Raven Press, New York. 207–232.
22. Warner, F. D., D. R. Mitchell, and C. R. Perkins. 1977. Structural conformation of the ciliary ATPase dynein. *J. Mol. Biol.* 114:367–384.
23. Witman, G. B., and N. M. Minervini. 1982. Dynein arm conformation and mechanochemical transduction in the eukaryotic flagella. *Symposium of the Association of Experimental Biology. In* Prokaryotic and Eukaryotic Flagella. W. B. Amos and J. G. Ducket, editors. Cambridge University Press. 203–223.
24. Heuser, J. E., and U. W. Goodenough. Three-dimensional structure of axonemal dynein. *J. Cell Biol.* 91(2, Pt. 2):49*a*. (Abstr.)
25. J. Wall. 1979. Biological scanning transmission electron microscopy. *In* Introduction to Electron Microscopy. J. J. Hren, J. I. Goldstein, and D. C. Joy, editors. Plenum Publishing Co., New York. 333–342.
26. Woodcock, C. L. F., L.-L. Y. Frado, and J. S. Wall. 1980. Composition of native and reconstituted chromatin particles: direct mass determination by scanning transmission electron microscopy. *Proc. Natl. Acad. Sci. U.S.A.* 77:4818–4820.
27. Mosesson, M. W., J. Hainfeld, J. Wall, and R. H. Haschemeyer. 1981. Identification and mass analysis of human fibrinogen molecules and their domains by scanning transmission electron microscopy. *J. Mol. Biol.* 153:695–718.
28. Freeman, R., and K. R. Leonard. 1981. Comparative mass measurement of biological macromolecules by scanning transmission electron microscopy. *J. Microsc.* 122:275–286.
29. Reedy, M. K., K. R. Leonard, R. Freeman, and T. Arad. 1981. Thick myofilament mass determination by electron scattering measurements with the scanning transmission electron microscope. *J. Muscle Res. Cell Motil.* 2:45–64.
30. Johnson, K. A., and J. S. Wall. 1982. The structure and molecular weight of 30S dynein from *Tetrahymena. Biophys. J.* 37(2, Pt. 2):345*a*. (Abstr.)
31. Johnson, K. A., and J. S. Wall. 1982. Structural and mass analysis of dynein by scanning transmission electron microscopy. *J. Submicrosc. Cytol.* In press.
32. Murphy, D. B., and R. R. Hiebsch. 1979. Purification of microtubule protein from beef brain and comparison of the assembly requirements for neuronal microtubules isolated from beef and hog. *Anal. Biochem.* 96:225–235.
33. Schiff, P. B., J. Fant, and S. B. Horwitz. 1979. Promotion of microtubule assembly *in vitro* by taxol. *Nature (Lond.).* 277:665–667.
34. Porter, M. E. 1982. Characterization of a native dynein and its interaction with microtubules. Ph.D. thesis. University of Pennsylvania, Philadelphia, PA.
35. Laemmli, U. K. 1970. Cleavage of structural proteins during the assembly of the head of bacteriophage T4. *Nature (Lond.).* 227:680–685.
36. Fairbanks, G., T. L. Steck, and D. F. H. Wallach. 1971. Electrophoretic analysis of the major polypeptides of the human erythrocyte membrane. *Biochemistry.* 10:2606–2617.
37. Amos, L. A., and A. Klug. 1974. Arrangement of subunits of flagellar microtubules. *J. Cell Sci.* 14:523–549.
38. Porter, M. E., and K. A. Johnson. 1982. ATP-sensitive binding of 30S dynein to bovine brain microtubules. *Biophys. J.* 37(2, Pt. 2):345*a*. (Abstr.)
39. Piperno, G., and D. J. L. Luck. 1979. Axonemal adenosine triphosphatase from flagella of *Chlamydomonas reinhardtii. J. Biol. Chem.* 254:3084–3090.
40. M. Takahashi, and Y. Tonomura. 1978. Binding of 30S dynein with the B-tubule of the outer doublet of axonemes from *Tetrahymena pyriformis* and ATP induced dissociation of the complex. *J. Biochem. (Tokyo).* 84:1339–1355.
41. Telzer, B. R., and L. T. Haimo. 1981. Decoration of spindle microtubules with dynein: evidence for uniform polarity. *J. Cell Biol.* 89:373–378.
42. Satir, P., J. Wais-Steider, S. Lebduska, A. Nasr, and J. Avolio. 1981. The mechanochemical cycle of the dynein arm. *Cell Motility.* 1:303–327.
43. Witman, G. B., K. A. Johnson, K. K. Pfister, and J. S. Wall. 1982. Fine structure and molecular weight of the outer arm dyneins of *Chlamydomonas. J. Submicrosc. Cytol.* In press.
44. Ogawa, K. 1973. Studies on flagellar ATPase from sea urchin sperm spermatozoa II. Effect of trypsin digestion on the enzyme. *Biochem. Biophys. Acta.* 293:514–525.

45. Cohen, C., and S. C. Harrison. 1971. X-ray diffraction from microtubules. *J. Mol. Biol.* 59:375–380.
46. Erickson, H. P. 1974. Microtubule surface lattice and subunit structure and observations on reassembly. *J. Cell Biol.* 60:153–167.
47. Mitchell, D. R. and F. D. Warner. 1981. Binding of dynein 21S ATPase to microtubules. Effects of ionic conditions and substrate analogs. *J. Biol. Chem.* 23:12535–12544.
48. Ponstingl, H., E. Krauhs, M. Little, and T. Kempf. 1981. Complete amino acid sequence of α-tubulin from porcine brain. *Proc. Natl. Acad. Sci. U.S.A.* 78:2757–2761.
49. Krauhs, E., M. Little, T. Kempf, R. Hofer-Warbinek, W. Ade, and H. Ponstingl. 1981. Complete amino acid sequence of β-tubulin from porcine brain. *Proc. Natl. Acad. Sci. U.S.A.* 78:4156–4160.